Copyright Warning & Restrictions

The copyright law of the United States (Title 17, United States Code) governs the making of photocopies or other reproductions of copyrighted material.

Under certain conditions specified in the law, libraries and archives are authorized to furnish a photocopy or other reproduction. One of these specified conditions is that the photocopy or reproduction is not to be "used for any purpose other than private study, scholarship, or research." If a, user makes a request for, or later uses, a photocopy or reproduction for purposes in excess of "fair use" that user may be liable for copyright infringement,

This institution reserves the right to refuse to accept a copying order if, in its judgment, fulfillment of the order would involve violation of copyright law.

Please Note: The author retains the copyright while the New Jersey Institute of Technology reserves the right to distribute this thesis or dissertation

Printing note: If you do not wish to print this page, then select "Pages from: first page # to: last page #" on the print dialog screen

ABSTRACT

SHOCK WAVE INTERACTION WITH A FLUID FILLED CYLINDER EXPERIMENTAL METHODS

by
Praveen Kumar Baba Siddabattuni

In the recent wars of Iraq and Afghanistan, many soldiers sustained bTBI (blast-induced traumatic brain injury). The blasts are created by extensive use of improvised explosive devices (IED's). Whether pure blast-shock waves cause TBI or what is the mechanism of injury are not fully known. Research efforts are underway to find answers to these questions.

The primary objective of this project is to understand how the shockwave interacts with a fluid-filled cylinder of different thicknesses. Here, the cylinder is idealized as head and the fluid filled inside it as the brain material. The primary interest here is, how the pure shockwave behaves when a cylinder is exposed to different incident blast over-pressures. The question raised in this work is whether primary blast wave causes for TBI? The pressure response inside the cylinder and the deformations for different thicknesses exposing at different blast loadings are taken into account in answering this question. Polycarbonate is chosen to simulate human skull. De-ionized water is used as the fluid as its mechanical property is close to that of brain. As the human head varies in thickness from 4mm in the temporal region to 8mm in the occipital region of the skull, two different thickness polycarbonate cylinders have been used to mimic that variation. All the experiments are done in the blast tube where the shockwaves are produced in the test section. Pure shock wave due to explosives in free field conditions will have a Friedlander wave form which will be artificially generated in 9 inch shock tube. High speed cameras

are used for capturing motion of the cylinder during shock loading.

Two different pressures 20 psi (140 kPa) and 30 psi (210 kPa) are used as the peak blast overpressures with two different thickness 1.9 and 3.3mm and diameter of the cylinder is 50mm. Pressure in the fluid is measured at three different locations whereas strain gages measure deformations at three sites.

Analysis of data indicate that the pressure in the fluid is affected by not only the external pressure but also thickness of the cylinder. Thus, the pressure is affected by both direct transmission as well as cylinder deformation.

SHOCK WAVE INTERACTION WITH A FLUID FILLED CYLINDER EXPERIMENTAL METHODS

by

Praveen Kumar Baba Siddabattuni

A Thesis
Submitted to the Faculty of
New Jersey Institute of Technology
in Partial Fulfillment of the Requirements for the Degree of
Master of Science in Mechanical Engineering

Department of Mechanical and Industrial Engineering

January 2016

APPROVAL PAGE

SHOCK WAVE INTERACTION WITH A FLUID FILLED CYLINDER EXPERIMENTAL METHODS

Praveen Kumar Baba Siddabattuni

Dr. Namas Chandra, Thesis Advisor Professor of Biomedical Engineering, NJIT	Date
Dr. Zhiming Ji, Committee Member Assoc. Professor of Mechanical Engineering, NJIT	Date
Dr. Shawn Chester, Committee Member Asst. Professor of Mechanical Engineering, NJIT	Date
Dr. Maciej Skotak, Committee Member Research Asst. Professor of Biomedical Engineering, NJIT	Date

BIOGRAPHICAL SKETCH

Author: Praveen Kumar Baba Siddabattuni

Degree: Masters in Science

Date: January 2016

Undergraduate and Graduate Education:

- Masters in Mechanical Engineering,
  New Jersey Institute of Technology, Newark, NJ, 2016

- Bachelor of Science in Aeronautical Engineering,
  Jawaharlal Nehru Technological University, Hyderabad, Telangana, India, 2013

Major: Mechanical Engineering

I dedicate this thesis work for all the people who read my thesis work and to all the soldiers throughout the world who sacrifice their lives for saving the people of their respective countries.

ACKNOWLEDGMENT

I would like to express my greatest gratitude to my advisor, Professor Namas Chandra for all his guidance, encouragement, and support throughout my graduate studies and also the sponsors who invest money for such kind of projects. I am deeply thankful for the opportunity to work in his laboratory and for his commitment to education and research. I would like to thank professors Zhiming Ji and Shawn Chester for being a part of the thesis defense committee.

I would also like to thank all the lab members (Matt, Maciej, Eren and Antony) from the Center for Injury Biomechanics, for their assistance, insight and support during various stages of my thesis.

Finally, I would like to express my gratitude to my Mom, Dad, Uncle and Aunt, and my friends without whom it would not have been possible for me to complete my master's thesis.

TABLE OF CONTENTS

TABLE OF CONTENTS
(Continued)

Chapter **Page**

TABLE OF CONTENTS
(Continued)

Chapter **Page**

LIST OF TABLES

LIST OF FIGURES

LIST OF FIGURES
(Continued)

LIST OF FIGURES
(Continued)

LIST OF FIGURES
(Continued)

CHAPTER 1

INTRODUCTION

1.1 Objective

The primary objective of this project is to investigate how a shockwave interacts with a fluid-filled cylinder. In this study, the cylinder represents a human head and the fluid filled inside it as the brain material.

Cylinders of two different thicknesses are exposed to blast loads at two different incident pressures to study effect of variation in thickness on pressure inside the cylinder. The questions needed to be answered are: a) does the variation in thickness of cylinder make any difference to the pressure inside the fluid and b) is deformation of the cylinder due to blast loads cause any effect on pressure applied inside the fluid? The fluid inside the cylinder has mechanical properties close to that of a human brain and acoustic velocity of polycarbonate cylinder is close to skull material. All the experiments are done inside a closed shock tube, which generates the experimental blast wave.

1.2 Background Information

Improvised explosive devices (IED's), the most common weapons used in wars, generate blast waves presumed to be the primary cause of TBI (1). According to symptoms presented following injury, the Glasgow coma scale categorizes the TBI into four types with scores of: Mild (13-15), Moderate (9-12), Severe (3-8) and Vegetative state (<3) (2). No skull fracture occurs in the mild case.

Experiments to comprehensively study the interaction of shockwaves with animals and PMHS (Post Mortem Human Subjects) are often expensive and require ample time; this project proposes alternative means to study this phenomenon (3).

A shock wave is formed when a disturbance is created in the medium which generates a wave travelling at supersonic speed (Mach>1). Shock waves will be distinguished into two categories according to their behavior: normal shock and explosive shock. In the former, the shock front will remain stationary to the observer and in the latter case the shock front will be dynamic (moving). In a normal shock, the domain before the formation of shock boundary has high velocity (greater than speed of sound) and low pressure. Alternatively, the domain after the shock boundary has low velocity (subsonic) and higher pressure than in the previous domain. For an explosive shock, the shock front will be moving in the direction of its burst in supersonic speed. The velocity considered in this case is the velocity of the shock front, whereas in the case of normal shock the velocity at the inlet (pre-shock) is considered (4). An example of normal shock is shock formation on wings of aircrafts travelling at supersonic speeds and for moving shock the best example is the shock wave generated due to explosions. In this project, the blast waves created are explosive shocks inside a closed test section, meaning the wave itself is moving in supersonic speed. Peak over pressure (highest point of pressure-time profile) values are used for analysis which are observed from sensors located at different known lengths in test section and their arrival times.

CHAPTER 2

EXPERIMENTAL SETUP AND DESIGN

In this chapter we will explore the design of the blast wave facility and the experimental setup which is used to determine the interactions of the shockwave on a circular cylinder.

2.1 Shock Tube

The shock tube is a closed tube where the shocks generated mimic the real shock waves generated from IED's. This shock tube consists of five main regions:

1. Driver Section
2. Membrane loading deck
3. Driven Section
4. Observation deck and
5. Back plate

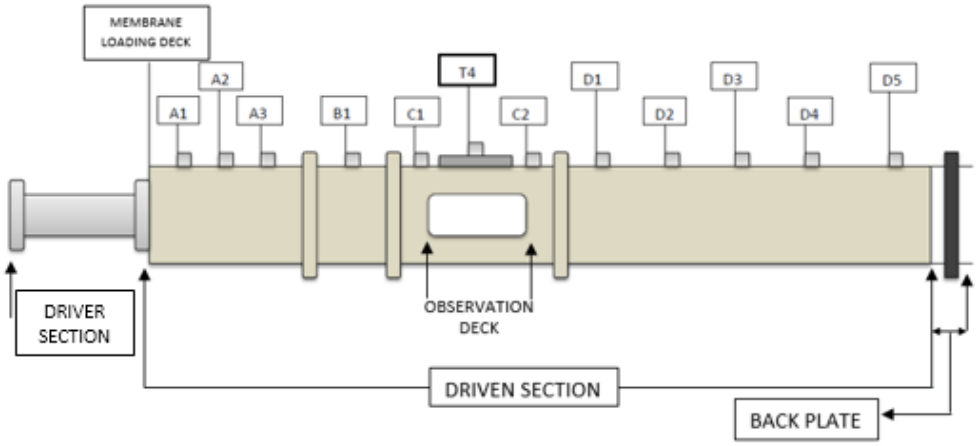

Figure 2.1 Shock tube schematic diagram.

Table 2.1 Sensor Distances from the Membrane Rupturing Location

Sensor	Distance from Membrane (m)
A1	0.66675
A2	0.92075
A3	1.42875
B1	2.11455
C1	2.6924
T4	3.07975
C2	3.4671
D1	3.9624
D2	4.4577
D3	4.98475
D4	5.5753
D5	5.842

2.1.1 Driver Section

The driver section is the breech where the highly pressurized gas (Helium or Nitrogen) will be filled. The driver section is connected to gas tanks by a pipe and the gas will flow inside the driver section, creating high pressure. This driver section will be completely closed while it is filled with compressed gas.

2.1.2 Membrane Loading Deck

A 0.01" thick Mylar membrane of different count will be placed in between driver section and test section. The number of membranes loaded depends on the desired intensity of the generated shock wave. By increasing the number of membranes, we increase the pressure required to rupture the membrane, known as the burst pressure.

2.1.3 Driven Section

The driven section has a 9” square cross section of 240” length and is made from stainless steel to survive the high pressure shock loading. This is where the shock waves travel following rupture of the membranes. The speed at which the shock wave travels is typically supersonic (Mach>1). Pressure sensors are placed at different locations at different lengths from membrane loading deck to obtain pressure-time profiles.

2.1.4 Observation Deck

The observation deck is where the test specimen will be experience the loading of the shock wave. This section is about 121.25” from the membrane loading deck. This deck has a bullet proof glass opening in order to withstand the blast loadings. A high speed camera which can record 5000 fps (frames per second) will be placed next to glass door to capture video data of what is happening to the specimen when exposed to shock wave.

2.1.5 End Plate

The primary purpose of this end plate is to stop the shock wave without causing damage to the surroundings. This end plate is placed with a gap from the test section to allow shock wave to leak through the gap. End plate is movable and can be placed at different lengths in order to avoid reflections which may reenter the test section. This reflected wave will cause the secondary rise in pressure in the pressure sensors.

2.2 Device Requirements

2.2.1 Kulite Pressure Transducer

Kulite sensors (model number: XCL-072-200A) were used to observe the dynamic pressures inside the cylinder. This model was chosen because it can read pressures up to 200 psi and is water resistant. It has thin lead wires which should be carefully arranged during the experiment, or else the shock loads may break the wire, if they are directly exposed.

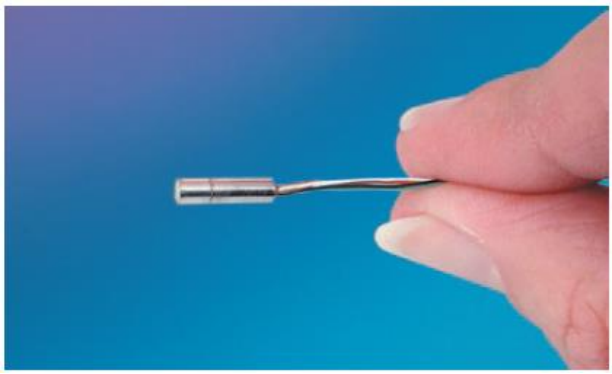

Figure 2.2 Kulite Pressure Transducer.
Source: Kulite XCL-072 series data sheet.

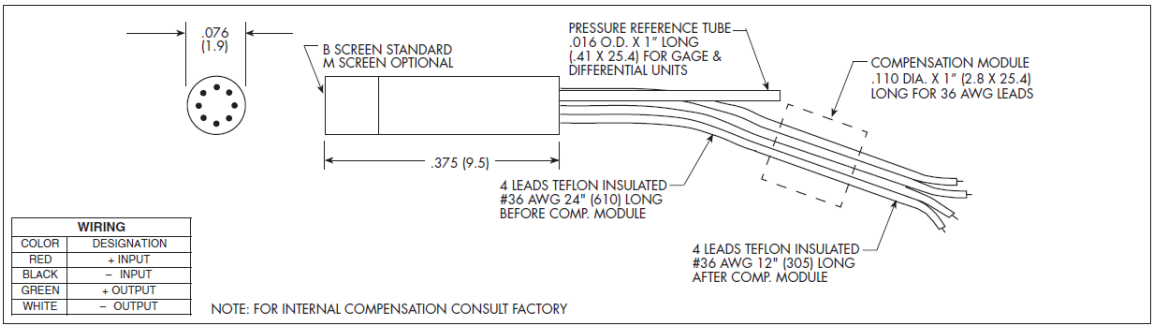

Figure 2.3 Dimensions and specifications of Kulite Sensor.
Source: Kulite XCL-072 series data sheet.

2.2.2 Stainless Steel Tubing

As the kulite metal lead length is just 10 mm, and cylinder diameter is 50 mm, it will be hard to keep them fixed inside the fluid without proper supports. Kulites are placed inside the cylinder by passing them through this tubing and placed at different lengths inside the cylinder. As we will be dipping this tubing inside the fluid there is the possibility of rusting. In order to avoid that, stainless steel tubing was selected.

Figure 2.4 Stainless steel tubing.
Source: McMaster Carr data sheet

2.2.3 Polycarbonate Cylinder

Transparent polycarbonate cylinder was selected as the test specimen because it has acoustic velocity close to skull material (Table 2.2, speed of sound). In these experiments, two thicknesses are selected (1.9mm and 3.3mm) to observe pressure variation inside the fluid with variable thickness. As the shockwave comes and loads the cylinder, the wave passes inside the cylinder differently for different thicknesses. This comparison will tell us how the wave interacts with the cylinder, i.e., how much wave is reflected and how much is transmitted inside the cylinder.

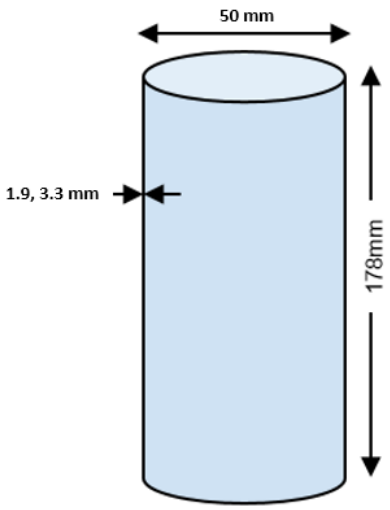

Figure 2.5 Cylinder Dimensions.

2.2.4 Slider Plates

The slider plates are used to keep the cylinder inside the test section. These plates are designed in such a way that the cylinder can either be fixed in all directions when exposed to shock waves or it can move in the direction parallel to the shock front (up to certain point). The end point is constrained by placing the screws from the side as shown in Figure 2.6 (b) such that the cylinder when comes and hits the screws will be completely stopped.

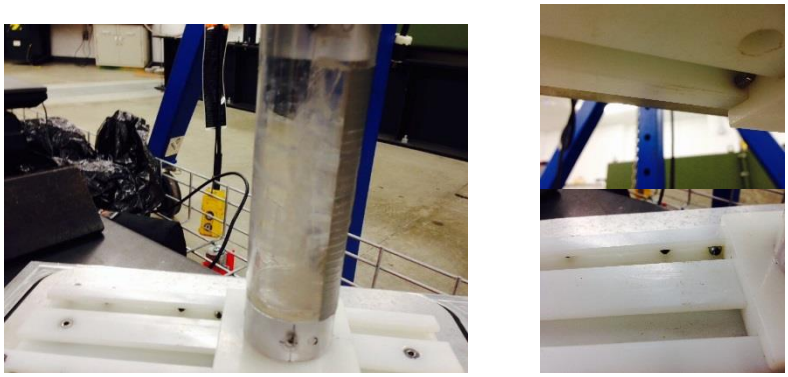

(a) **(b)**

Figure 2.6 (a) Slider plates with cylinder (b) Top and bottom screws to fix end point.

2.3 Cylinder Setup for Experiment

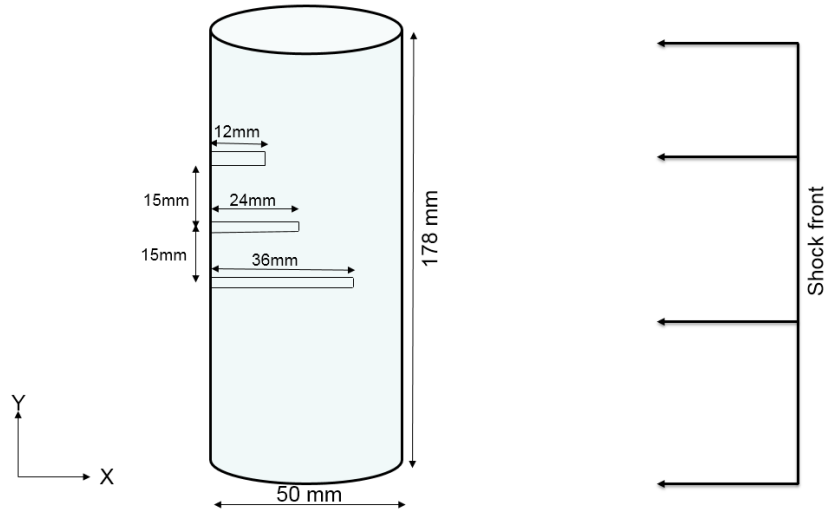

Figure 2.7 Dimensions of the cylinder and the sensor location with respect to shock front.

The polycarbonate cylinder is placed inside the test section with top and bottom surfaces attached to plates which are made to move in only one direction. Both plates are made in such a way that the cylinder will stop sliding at some particular point as per the location of the stopper screws. The fluid used inside the cylinder is deionized water which has mechanical properties similar to that of brain material.

Table 2.2 Material Properties of Different Materials

Material	Density (Kg/m^3)	Elastic Modulus (Mpa)	Speed of sound (m/s)
Skull	5370	5370	2900
Polycarbonate	1220	2380	2270
Brain material	1040	2190	1509
Water	1000	2400	1482

2.4 Pre-Experimental Considerations

2.4.1 Sealing of the Cylinder

Since there is fluid inside the cylinder exposed to high pressure conditions, there is a chance of fluid leakage. In order to avoid that, a small layer of ballistic gel is used to seal the bottom of the cylinder. The ballistic gel used is made from 20 % silicone powder and was mixed with water to make it in solid form at room temperature, able to transform back to a viscous fluid when heated. The ballistic gel was heated and, after closing the bottom cap, this gel is poured from the top of cylinder forming an 8 mm thick layer. After sealing it with the gel, we filled it with water and observed the presence or absence of leakages for 24 hours.

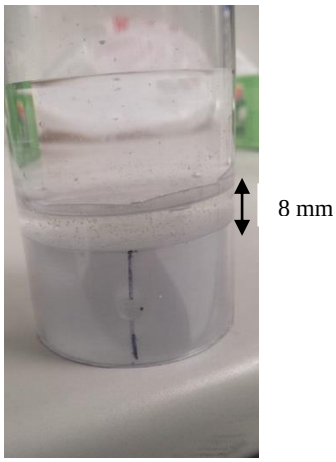

Figure 2.8 Sealing of the cylinder bottom with ballistic gel.

2.4.2 Dummy Sensor Test

The dummy sensor test was done to test whether the actual sensors would survive the blast loadings when placed inside the water-filled cylinder. We kept the dummy sensors at different lengths inside of the cylinder, leaving wire tips exposed in the direction of the shock wave and mounted them inside the fluid using stainless steel tubing.

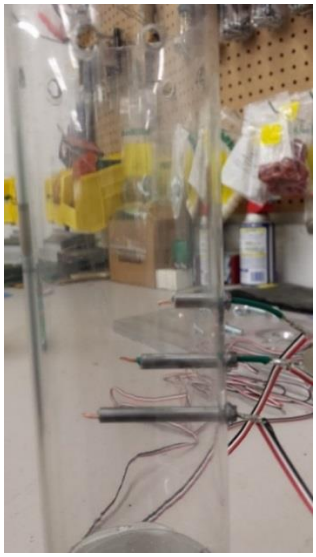

Figure 2.9 Dummy sensors placed inside the cylinder oriented at different lengths.

After exposing the dummy sensors to shock wave, no damage was observed at an incident pressure of 27 psi blast loading conditions. The stainless steel tubings were placed by drilling a hole on the back of cylinder and used Loctite adhesive to both seal and tightly fix the conduits.

2.4.3 Pre-Experimental Test Shot – All Pressure Sensors in Same Plane

The pre-experimental test has been done by placing all sensors on same distance in X direction, so that when the shock wave comes and loads the cylinder, some part of the wave is transmitted into the cylinder and some part of the wave will be reflected back due to impedance mismatch. The main purpose of this experiment is to observe peak pressure value observed inside the cylinder and to check whether the arrival times of all kulite sensors are equal.

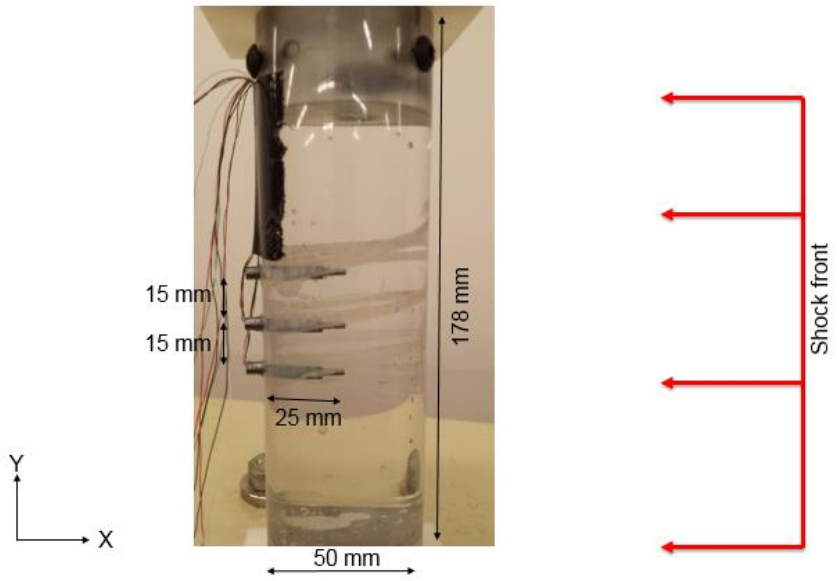

Figure 2.10 Experimental setup with sensors placed in the same plane (at the center).

When we did this pre-experimental test, we have observed a lot of noise in the signal which overlaps the original signal. After the shock wave passes the cylinder, the cylinder will compress and expand (bulging effect) which may be the source of the noisy signal. This presented an important question: is the signal quality noisy due to its electrical components or due to the bulging effect of the cylinder.

2.4 FFT Analysis and FFT Filtering

In order to observe the original signal and remove the noise signal from the output, FFT (Fast Fourier Transform) Analysis has been done for the output. When FFT is applied for the signal, it converts the signal from its time domain to frequency domain. After considering the output generated from the FFT analysis, from Figure 2.10 (a), lot of noise observed at different frequency levels. In order to remove noise effects from the signal

without losing original output, 10 KHz low pass filtering was done. The unfiltered signal and the filtered signal for one of the sensor is shown in the Figure 2.11.

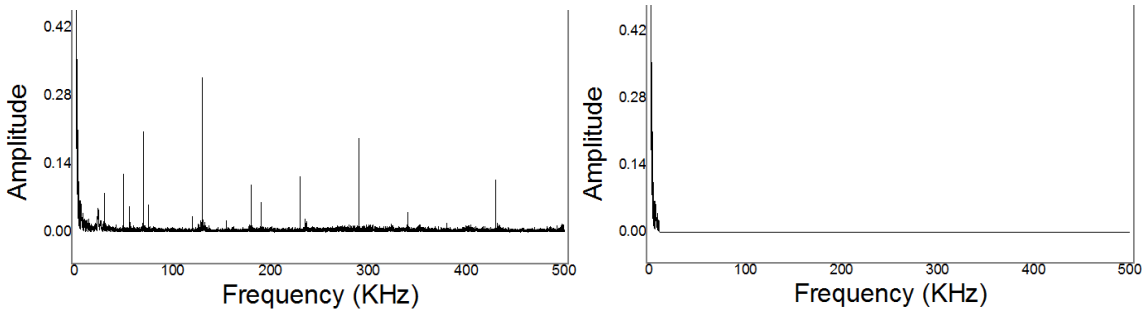

(a) **(b)**

Figure 2.11 FFT output- Frequency domain (a) Before filtering, (b) After filtering for one of the sensor.

In order to remove the noise disturbance from the signal, low pass filtering has been done by selecting appropriate frequency according to the output amplitude from FFT analysis. Usually 10 KHz low pass filtering will be a good filtering frequency point and all the filters used in these graphs are done using this level.

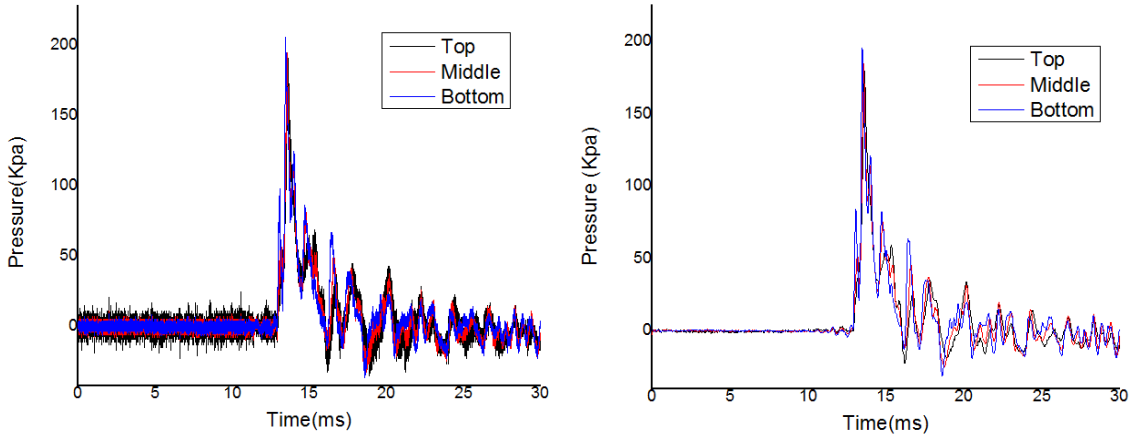

(a) **(b)**

Figure 2.12 Signal filtering (a) before filtering-Actual output (b) low pass filtered signal at 10 KHz.

2.6 Theoretical Considerations

2.6.1 Moving Cylinder Assumptions

The cylinder is set to move freely up to a certain point in the shock tube to create free field conditions of blast, similar to how specimens are free to move when shock waves interact with them. In the shock tube, it is difficult to unconstraint the specimen in all three directions thus only the direction parallel to the shock wave is made free to move up to certain point. The stationary cylinder tests have been designed in order to prove that the cylinder is absorbing more deflections from the shock wave and that deflection is indirectly causing more vibrations on the wall of cylinder, and in turn, transmitting those vibrations to the wall mounted steel tubing and overlap with the signal output observed.

The moving cylinder will also observe some vibrations due to shock loads applied on the cylinder, but when compared to the stationary cylinder it was less than the stationary case. This is because maximum bending will occur when the cylinder is completely fixed in both the ends; all the shock loads will cause greatest deformation at the center. But when we consider the cylinder to be moving, some of the energy is used to move the cylinder and only some part of energy will be absorbed by the cylinder.

2.6.2. Shock Wave Theory

Before the moving shock front, all conditions were taken to be the same as ambient conditions. After the shock front there will high pressure, low temperature and high velocity (Mach>1). The shock front is infinitesimally small layer and the pre-shock and post-shock conditions are valid within the boundary layer of the shock front. As the

change in state across the shock front is almost instantaneous, it is considered to be adiabatic process (no heat transfer).

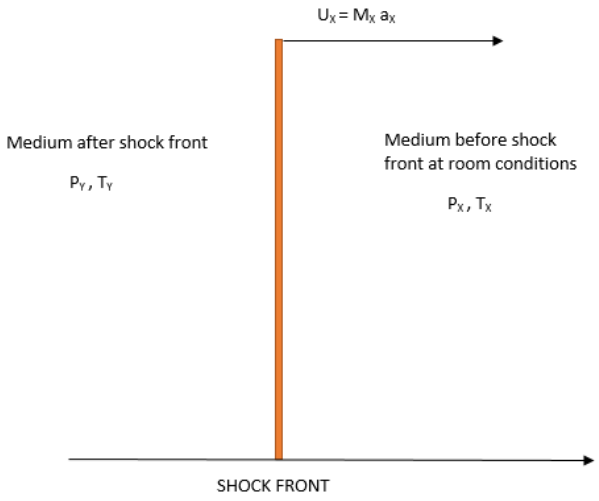

Figure 2.13 Explosive shock boundary conditions.

$$\mathrm{M}_x = \frac{U_\mathrm{x}}{a_x} \tag{2.1}$$

$$a_x = \sqrt{\gamma \mathrm{RT}} \tag{2.2}$$

$$\mathrm{M}_y = \sqrt{\frac{5 + {\mathrm{M}_x}^2}{7{\mathrm{M}_x}^2 - 1}} \tag{2.3}$$

$$\frac{P_y}{P_x} = \frac{7{\mathrm{M}_x}^2 - 1}{6} \tag{2.4}$$

$$\frac{T_y}{T_x} = \frac{(5 + {\mathrm{M}_x}^2)(7{\mathrm{M}_x}^2 - 1)}{36{\mathrm{M}_x}^2} \tag{2.5}$$

For an ideal gas, the above Rankine- Hugoniot equations can be used to obtain the theoretical values of aftershock pressure and temperatures. Here M_x is the Mach number of the explosive shock, a_x is the acoustic velocity of the medium which depends on γ specific heat ratio of the medium, R is the universal gas constant, T is the absolute temperature, M_y is the Mach number aftershock medium, P_x is the pressure before shock and will be considered to be atmospheric pressure, P_y is the pressure at a point in the medium aftershock, T_x is considered as room temperature and T_y is the temperature after the shock medium. The specific heat ratio, γ of air is approximately 1.41 and the universal gas constant R for air is approximately 287 J/ (Kg*K). If we know only the velocity of the shock front, we can calculate all the pressure and temperatures after the shock (4).

2.6.3. Direct and Indirect Loads

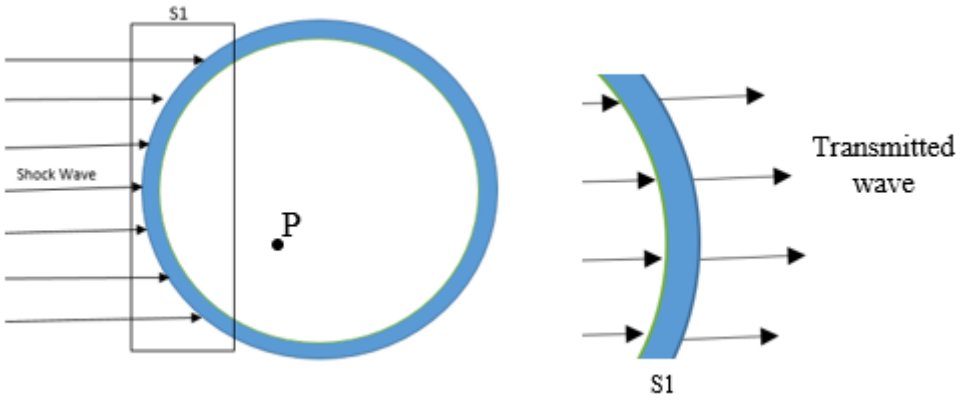

Figure 2.14 Indirect loads applying on cylinder (a) At time t=0 when shock front comes and hits the cylinder (b) S1- At time t when the wave transmission takes place inside the cylinder after compression of cylinder.

When the shock wave comes and hits the cylinder, there will be two kinds of loads applied inside the fluid: direct loads due to the transmitted wave inside the fluid (fluid pressure) and the indirect loads due to the compression of the cylinder. The data recorded from the pressure sensors mounted inside the cylinder are a result of both these loads. So if we consider a point inside the fluid as P, then

$$P = P_D + P_{ID} \tag{2.6}$$

Where P_D is pressure due to direct load of the shock front transmitted inside the fluid and P_{ID} is due to the compression of the cylinder due to shock loads. The intensity of the transmitted wave between two different media depends upon the acoustic impedance of the media (5, 6).

$$\sigma_t = \sigma_i\left(\frac{2Z_{\Omega A}}{Z_{\Omega B} + Z_{\Omega A}}\right) \tag{2.7}$$

where σ_t is wave transmitted between two mediums A and B. In this case A is the medium before interaction and B is medium after interaction. σ_i is the incident wave impinging on the interface between A and B. $Z_{\Omega A}$ and $Z_{\Omega B}$ are acoustic impedance of medium A and medium B.

Table 2.3 Acoustic Impedance of Different Materials (7)

Material	**Density (Kgm^{-3})**	**Speed of Sound (ms^{-1})**	**Acoustic Impedance ($Kgm^{-2}s^{-1}x10^{-6}$)**
Air	1.3	330	0.000429
Polycarbonate	1220	2270	2.76
Water	1000	1450	1.45
Skull	1710	2900	4.95

Theoretically, from transmitted wave between air and polycarbonate is calculated as twice the incident pressure and from polycarbonate to water transmitted wave will be 0.69 times the incident pressure.

The transmitted wave inside the fluid will travel faster than when it is in air because passage of information between the particles is quicker in thicker medium than in thinner medium (4). While the shock wave travels at a speed of 330 m/s at room temperature, once it is transmitted into the cylinder the shock will travel at a speed of 1450 m/s. Likewise, the wave transferred to the cylinder wall (polycarbonate) will travel at a speed of 2270 m/s which is called the stress wave due to shock loads.

2.7 Pure Shock Wave Behavior inside the Shock Tube

In a free field blast the intensity of the shock wave will be gradually decreasing as we move further and further away from the exploded region. The pressure varies depending upon time and distance. The shock tube we have in our lab is able to generate pure shock loading conditions.

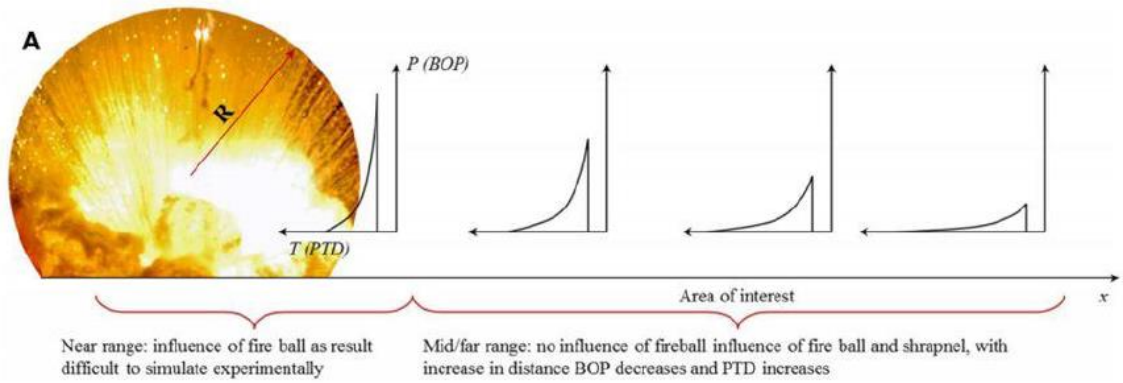

Figure 2.15 Blast wave profile decreasing with the increase of distance from exploded region (8).

If we consider the explosion expands spherically with a radius of R, then within that radius it is difficult to calculate the blast over pressures due to the debris formed due

to explosion. After certain distance, there won't be any effect of the fire ball formed due to explosion and a pure Friedlander wave form can be achieved.

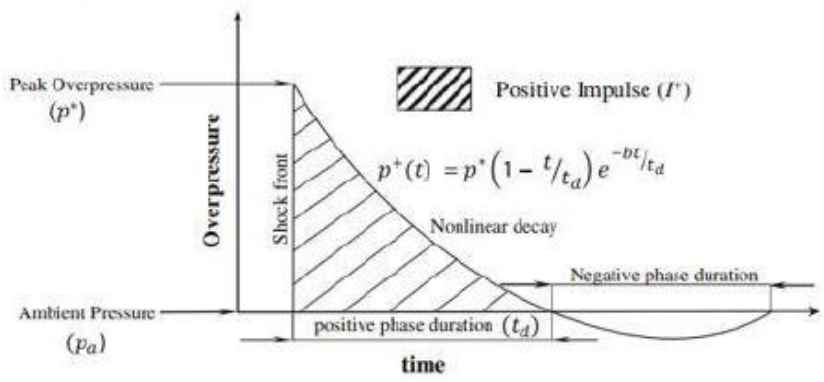

Figure 2.16 Friedlander wave form (9).

Consider:

$$p\,(t) = p_o\left(1 - \frac{t}{t_d}\right)e^{\left(\frac{-t}{\alpha}\right)}$$

where p_o is the blast over pressure, t_d is the positive time duration and α is the delay constant (9). Achieving Friedlander wave in lab conditions might vary slightly form original free field conditions due to reflections from ground and surrounding buildings.

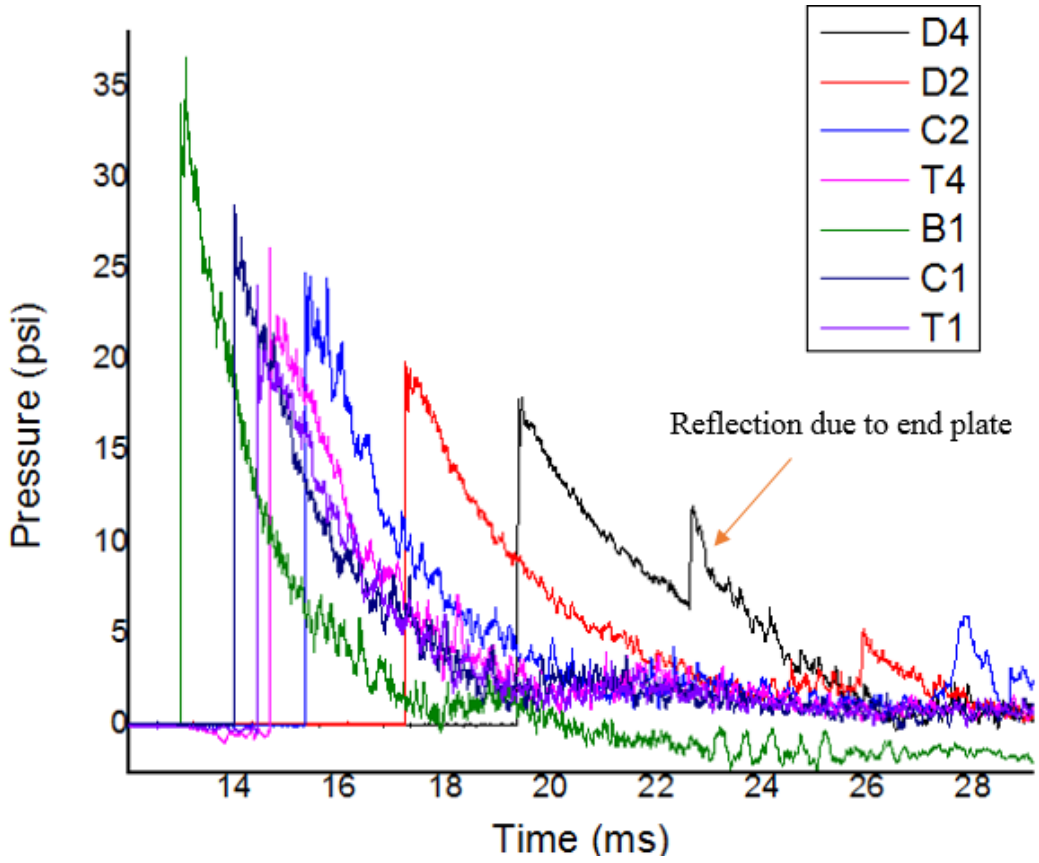

Figure 2.17 Friedlander wave generated from the sensors located at different distances in shock tube.

The pressure intensities are getting lower as we move away from the membrane rupture area, while still achieving Friedlander wave forms. When there is an offset plate close to the test section, some part of the shockwave will be reflected back into the test section and this causes the secondary rise in pressure value (4), as seen from sensor D4 (this is the sensor located closest to the end plate).

Table 2.4 Theoretical and Experimental Difference for C1 Sensor Peak over Pressure values.

No. of Membranes	Theoretical (psi)	Experimental (psi)	% error
2	25.46	22.85	10.25
4	34.41	37.93	10.25
6	59.31	56.36	4.96

The error percentage observed for C1 sensor located near to the observation deck shows that the difference between the theoretically calculated values using the Rankine Hugoniot equations (4) show approximately 5-10% error as the theoretical values of those equations are valid for ideal gas and that difference is negligible when we compare them with real gases.

Although, it has not been completely proved that the peak value obtained experimentally is because of pure shock wave, experiments are being done to investigate that. When the membrane ruptures, shock front travels in the direction of driver section to driven section, at the same time another expansion wave will be generated which travels in opposite direction of shock front. This expansion wave will travel faster than shock front because, shock front will travel in a medium which is in atmospheric condition, but the expansion wave will be travelling in the medium which is already being compressed. Assumption is that, the peak values obtained from the sensors (Figure 2.17) is due to both expansion wave and the shock wave.

CHAPTER 3

RESULTS AND DISCUSSION

The readings from the sensors used and the shock wave behavior inside and outside the cylinder are discussed in the following chapter. Each graph will be discussed following the related figures.

3.1 Moving Cylinder- Pressure Sensors on Same Plane

A test using a moving cylinder (1.9 mm thick, 50 mm dia) with pressure sensors placed on the same location was done to test if all the Kulite pressure sensors respond at the same time and to observe homogeneity in the outputs of all the sensors. The cylinder is allowed to move in X direction, parallel to the shock wave, and an endpoint is fixed in the slider plate so that the cylinder can move 2.5in from the place it is fixed before the exposure to shockwave.

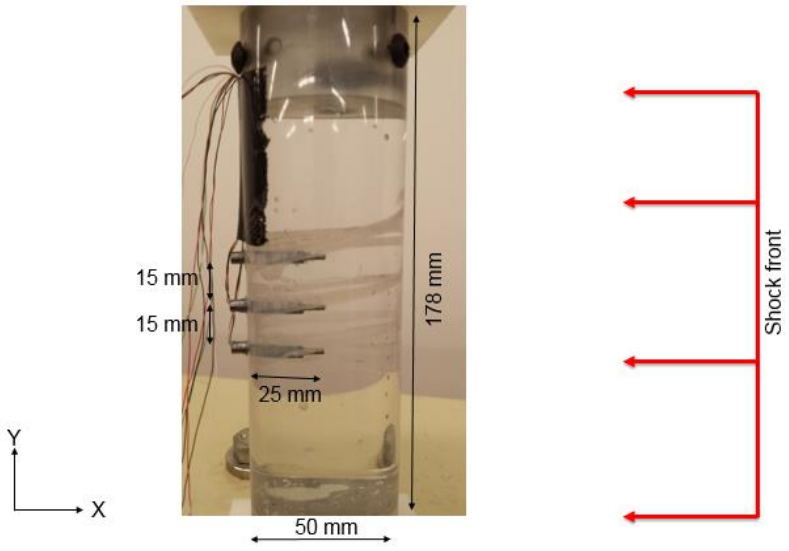

Figure 3.1 Orientation of the Kulite probes kept on same distance in X-Direction and 15 mm apart in Y-Direction.

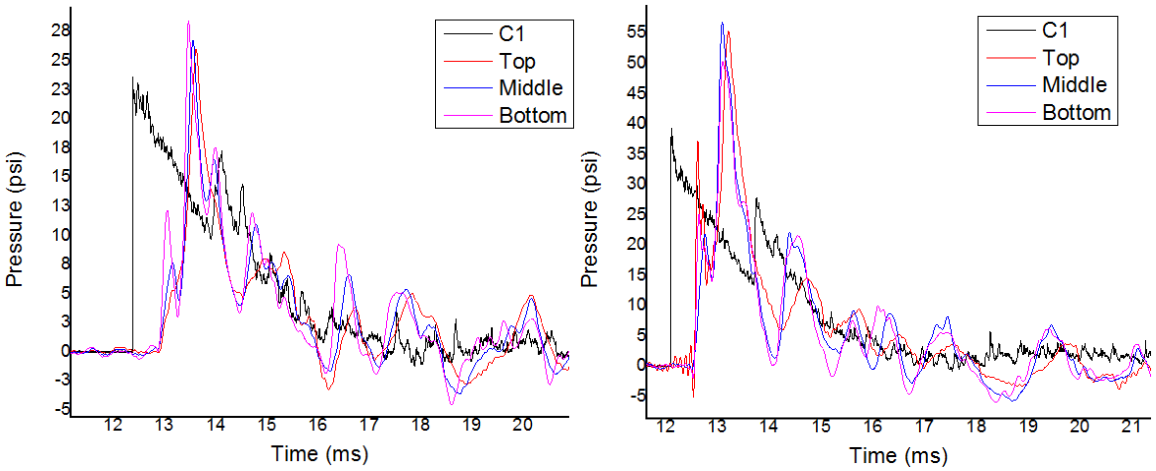

Figure. 3.2 Kulites placed on top, middle and bottom response to shock loads at incident Pressure of approximately (a) 16 psi (b) 27 psi

When the kulites were placed on same plane, the arrival times of the pressure sensors responded almost concurrently with a minimal difference of approximately 0.005 milliseconds. The primary peak pressure is due to the shock wave transmitted into cylinder and secondary peak is due to maximum deformation of cylinder. After the secondary peak, the zigzag pattern of the graph is due to the bulging effect of the cylinder. When the polycarbonate cylinder filled with water is subjected to blast loads; since the polycarbonate is plastic material, it will continuously contract and expand (Compression and Tension). When the walls compress in the front and back, the fluid is pushed towards the Kulite pressure sensing area which reads the positive pressure readings. When the cylinder wall tries to move back to its original position, the fluid will separate from the wall of the cylinder, causing a negative dip in the graph. This happens for a certain period of time until all the energy that has been transferred from the shock wave to the cylinder disappears. For the moving cylinder, although all the secondary peaks due to deformation are equal, the primary peak which is due to transmission of shock to fluid seems to be varying slightly. In order to check the energy transferred from

blast loads to the fluid-filled cylinder, impulse (area below the graph) for a certain time period (40 ms), where the deformation of the cylinder shows almost no variation, has been calculated by considering only the positive phase of wave as shown in Figure 3.3. For comparison, for top, middle and bottom placed sensors at two incident pressures, there seems not much difference in energy transmitted from the blast wave to cylinder. The energy is equally distributed in Y direction as we have placed the cylinder at equal lengths in X direction.

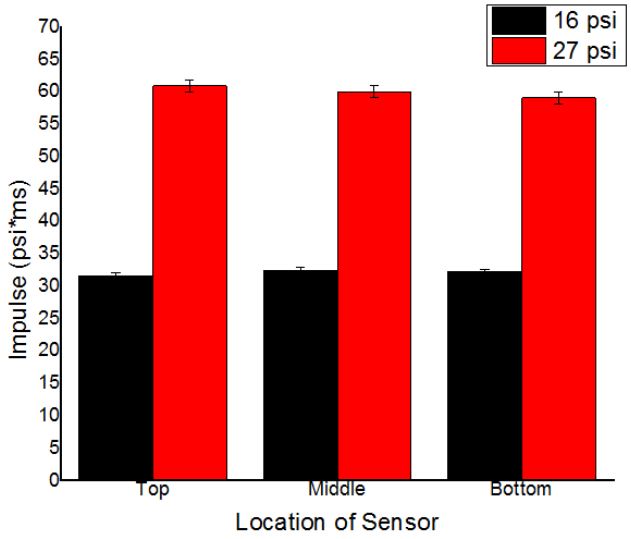

Figure 3.3 Impulse graph comparison for the moving cylinder at different incident pressures.

3.2 Stationary Cylinder- Pressure Sensors on Same Plane

The stationary cylinder pressure sensor test was done to observe the bending effect of the cylinder (1.9 mm, 50 mm dia) upon the kulite sensors oriented in the same plane. If the cylinder is kept stationary, then the loads due to blast will be directly applied on the polycarbonate cylinder causing increased bending. Our interest is the pressure response

due to the bending of the shockwave. The cylinder is kept fixed on the slider plate at the end point (close to T1 sensor) in the shock tube so that it cannot move.

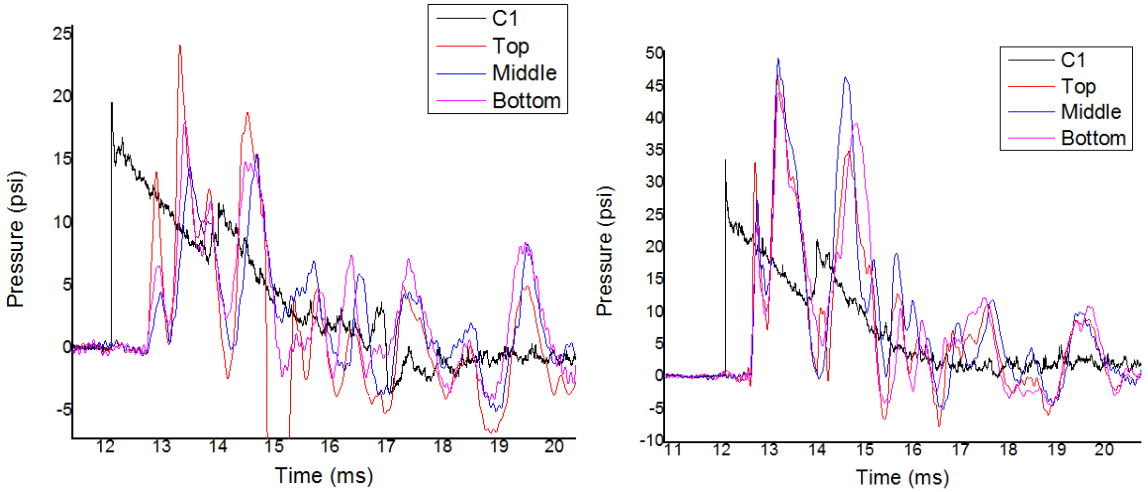

(a) **(b)**

Figure 3.4 Stationary cylinder kulite readings with incident pressures (a) 16 psi (b) 27 psi.

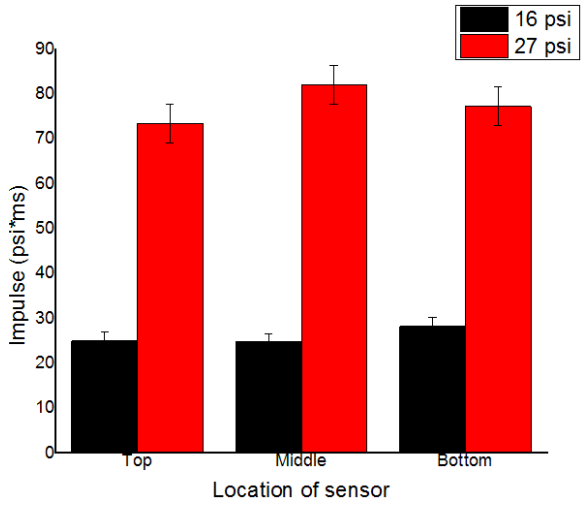

Figure 3.5 Impulse graph comparison for the stationary cylinder at different incident pressures.

From the graphs above, although the arrival times of all the Kulite sensor readings are similar, the peak pressure values are inconsistent, as expected. The deformation of the cylinder plays a key role in the mismatching of the peak pressure values. The primary peak from the graph is due to the shock loads, the secondary peak is due to deformation

of the cylinder and the third peak due to the compression and expansion effect of cylinder. Notice that this peak is so high that it almost equals the secondary peak. This high compression is due to the stationary position of the cylinder that completely absorbs the blast loads which is low in case of moving cylinder.

In order to check that the energy transferred from the shock to the cylinder is due to direct and indirect loads, impulse has been calculated for both the shots at different incident pressures by, eliminating the negative portion due to tension of the cylinder. If we consider the graph from arrival time to 40ms, we can observe that the impulse of the positive signal is consistent in sensors positioned on top, middle and bottom of cylinder. For the incident pressure of 16 psi, the impulse of the three sensors ranged from 25 to 30 psi-ms and for the incident pressure of 27 psi, the impulse reading of the kulite sensors ranges from 75 to 80 psi-ms. This difference may be due to the minimal change in lengths of kulites inside the cylinder. Considering that we are observing supersonic shock velocities, even this small change in length can have a significant effect on the observed pressure-time profiles.

3.3 Thin Cylinder Exposed to Shock Wave

A thin polycarbonate cylinder, which is representative of a human skull, of 1.9 mm and 50 mm diameter has been exposed to shock wave with strain gauges attached on the front, side and back of cylinder. Deionized water has been idealized as brain and was used to fill the cylinder. The response of the sensors, located 12mm apart, will be considered to calculate the velocity at which the shock wave is travelling inside the cylinder.

When a shock wave comes and interacts with the cylinder, there are two types of waves generated between different mediums: a) the stress wave which passes through the wall of the cylinder and b) pressure wave which is transmitted to the fluid from the polycarbonate wall. The stress wave will result in deformation of the cylinder, which causes the indirect loads applied inside the fluid and the direct load due to transmitted wave inside the fluid.

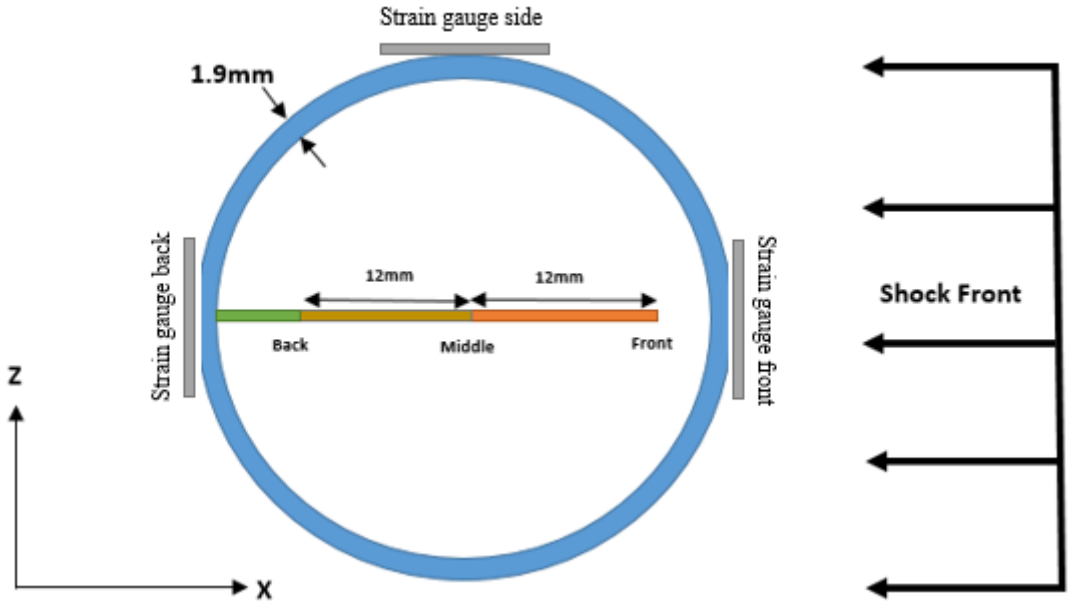

Figure 3.6 Thin Cylinder- Top view of the cylinder, Kulite sensors location and distance between them.

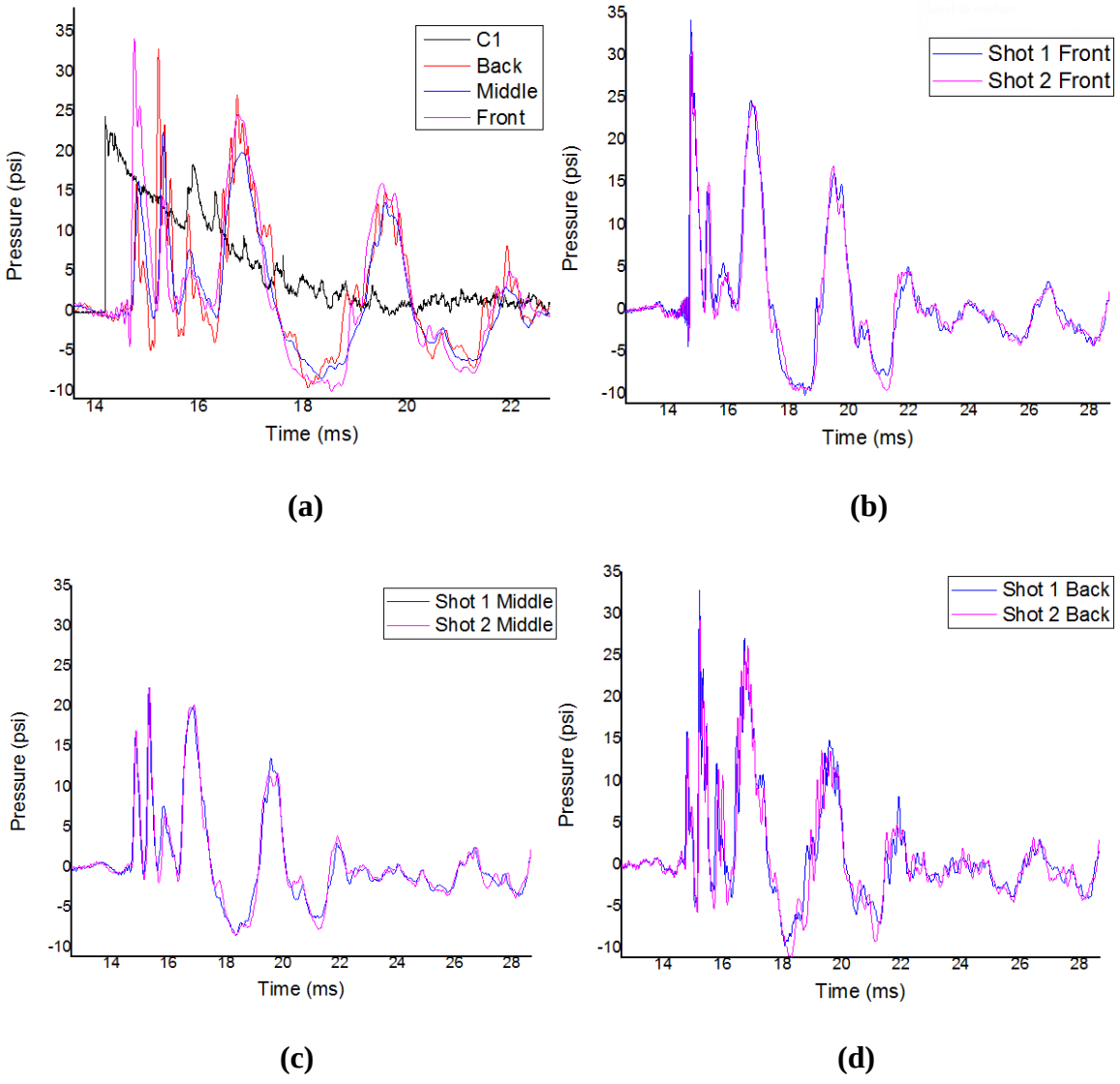

Figure 3.7 Thin cylinder- For incident pressure of 20 psi, pressure profiles of sensors (a) C1, Back Front and Middle (b) Front sensor response (c) Middle sensor response (d) Back sensor response for two samples.

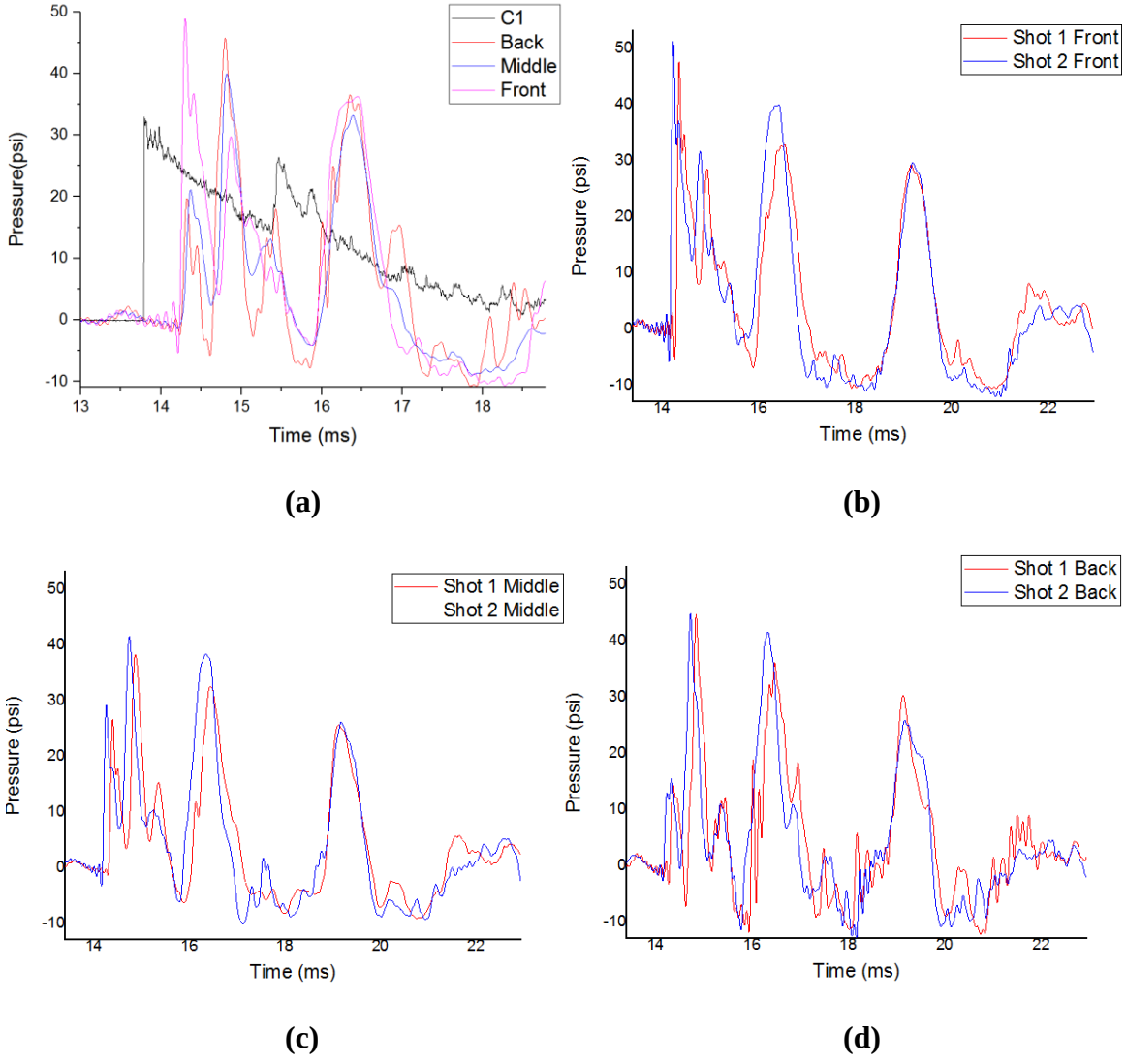

Figure 3.8 Thin cylinder- For incident pressure of 30 psi, pressure profiles of sensors (a) C1, Back Front and Middle (b) Front sensor response (c) Middle sensor response (d) Back sensor response for two samples.

From Figure 3.6 (a), for incident pressure of 20 psi the front, middle and back sensors follow the same trend and expected peak values. The transmitted pressure wave from the cylinder to the fluid loses its intensity as it enters into the fluid. The primary peak value, due to the resulting fluid pressure, is transmitted from the cylinder due to shock loads. This wave reduces its intensity from approximately 34 psi in the front sensor to 17 psi in the middle and 14 psi in the back. The secondary peak value increases from the front sensor to the back sensor due to the deformation of the cylinder and consequent indirect loads applied inside the fluid. The secondary peak value has been increasing from 15 psi in the front, to 23 psi in the middle and 30 psi in the back of the cylinder.

Despite the sensor locations, maximum deflection applies at the center. The front sensor is fixed at the bottom of the cylinder and its tip is placed close to the cylinder wall, which results in less deflection loading. From Figure 3.7 (a), for incident pressure of 30 psi, the front, middle, back sensors also follow the same trend due to direct and indirect loads applied on the cylinder. For comparison the C1 sensor, the closest sensor before the observation deck, is also included. As the incident pressure is increased from 20 psi to 30 psi, the primary peak value (due to the transmitted wave) and the secondary peak (due to the indirect loads) also increased. The primary peak value reading from front sensor is observed to be approximately 48 psi, decreases to 29 psi and, when it reaches the back sensor, 15 psi. The secondary peak value has increased from 30 psi in the front sensor, to approximately 40 psi in the middle sensor and further increased to 44 psi in the back sensor.

The secondary peak value of front, middle and back sensors for 30 psi incident pressure is greater compared to 20 psi readings because, as the blast loads increases the deformation in the cylinder increases thereby increasing the indirect loads applied inside the fluid.

Table 3.1 Arrival Time Chart for Thin Cylinder at Different Incident Pressures

Incident Pressure (psi)	Arrival Time (ms)		Time Difference (s)x 10^{-5}	Distance (m)	Velocity (m/s)
	Front	Middle			
20	14.7010	14.7120±0.002	1.1	0.012	1090±150
30	14.3136	14.3230±0.003	0.94	0.012	1276±300

Arrival times are based on the time at which the sensors start responding. In Table 3.1, the arrival times of front Kulite and middle Kulite at different known distances are considered to calculate the experimental values of velocities at which the shock wave travels inside the fluid (Fluid Pressure). These arrival times are taken as the time of the primary peak from Figure 3.7. The acoustic velocity of water is 1482 m/s (at room temperature) and velocity, calculated from arrival times of the sensors, is observed to be approximately equal.

3.4 Thick Cylinder Exposed to Shock Wave

Thick cylinder of 3.3 mm of same diameter as thin cylinder (50 mm) is considered to analyze the effect of thickness on variation in pressure inside the fluid. For the thick cylinder, only two sensors are used as one of the Kulite sensor was broken due to repeated exposure to blast loads. The two Kulites are positioned in the front and the back, facing the shock front with an inter-sensor distance of 24 mm. To observe the deformations, three strain gauges are placed on the front (exposed directly to shock front), on the side and on the back of cylinder - exactly at the center of the cylinder where maximum deflection is observed.

The hypothesis is that deformations should be lower in the thick cylinder than the thin cylinder. The indirect load-dependent pressures should be lower in the kulite pressure readings.

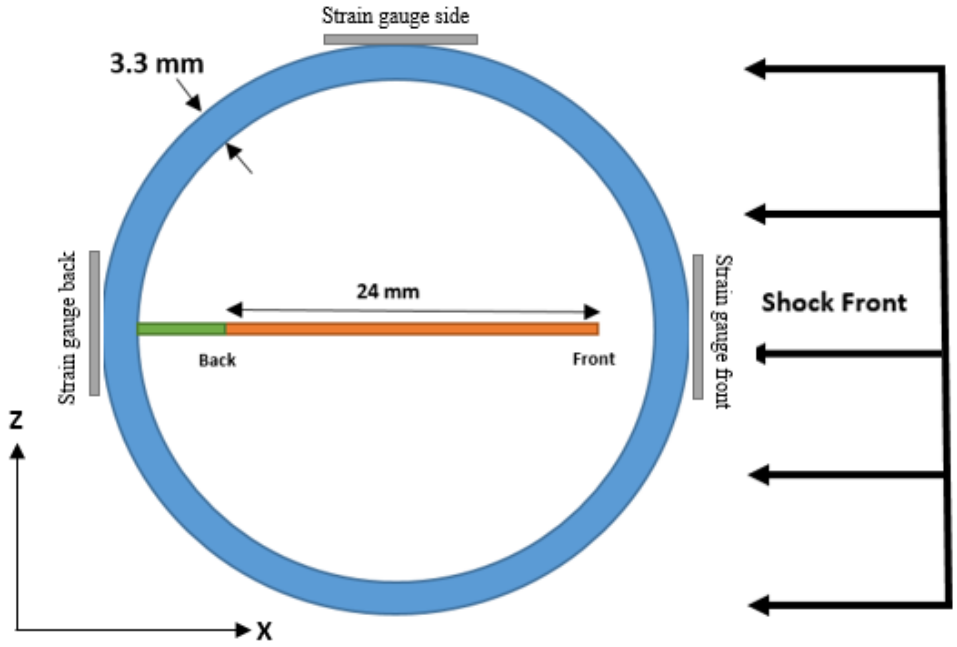

Figure 3.9 Thick Cylinder- Top view of the cylinder, Kulite sensors location and distance between them.

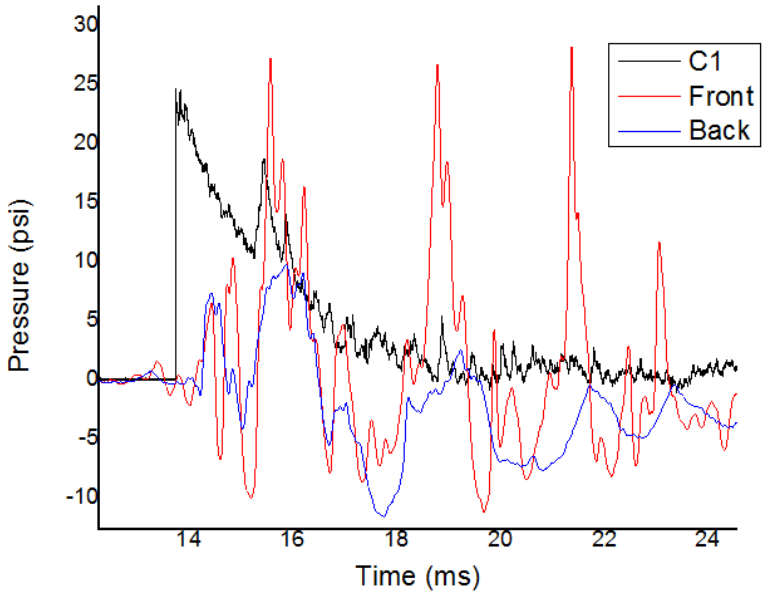

(a)

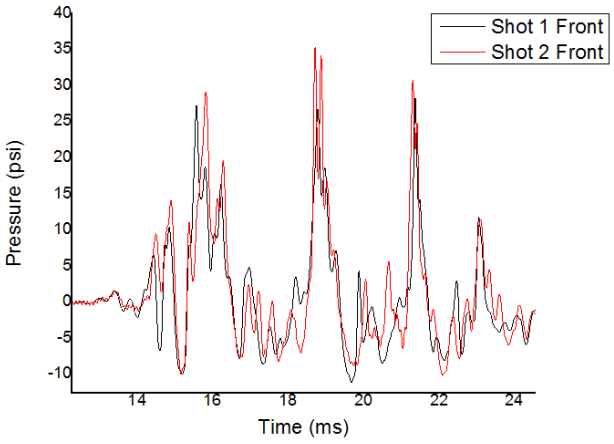

(b)

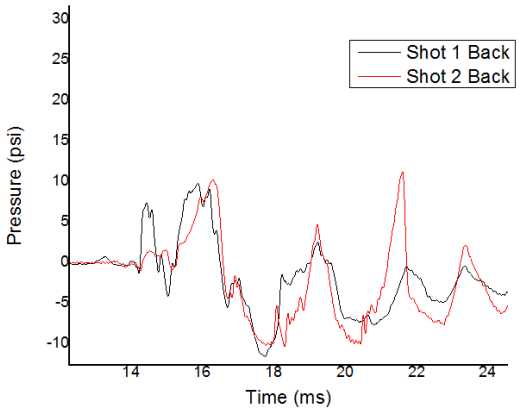

(c)

Figure 3.10 Thick cylinder- For incident pressure of 20 psi, pressure profiles of sensors (a) C1, Front and Back (b) Front sensor response (c) Back sensor response for two samples.

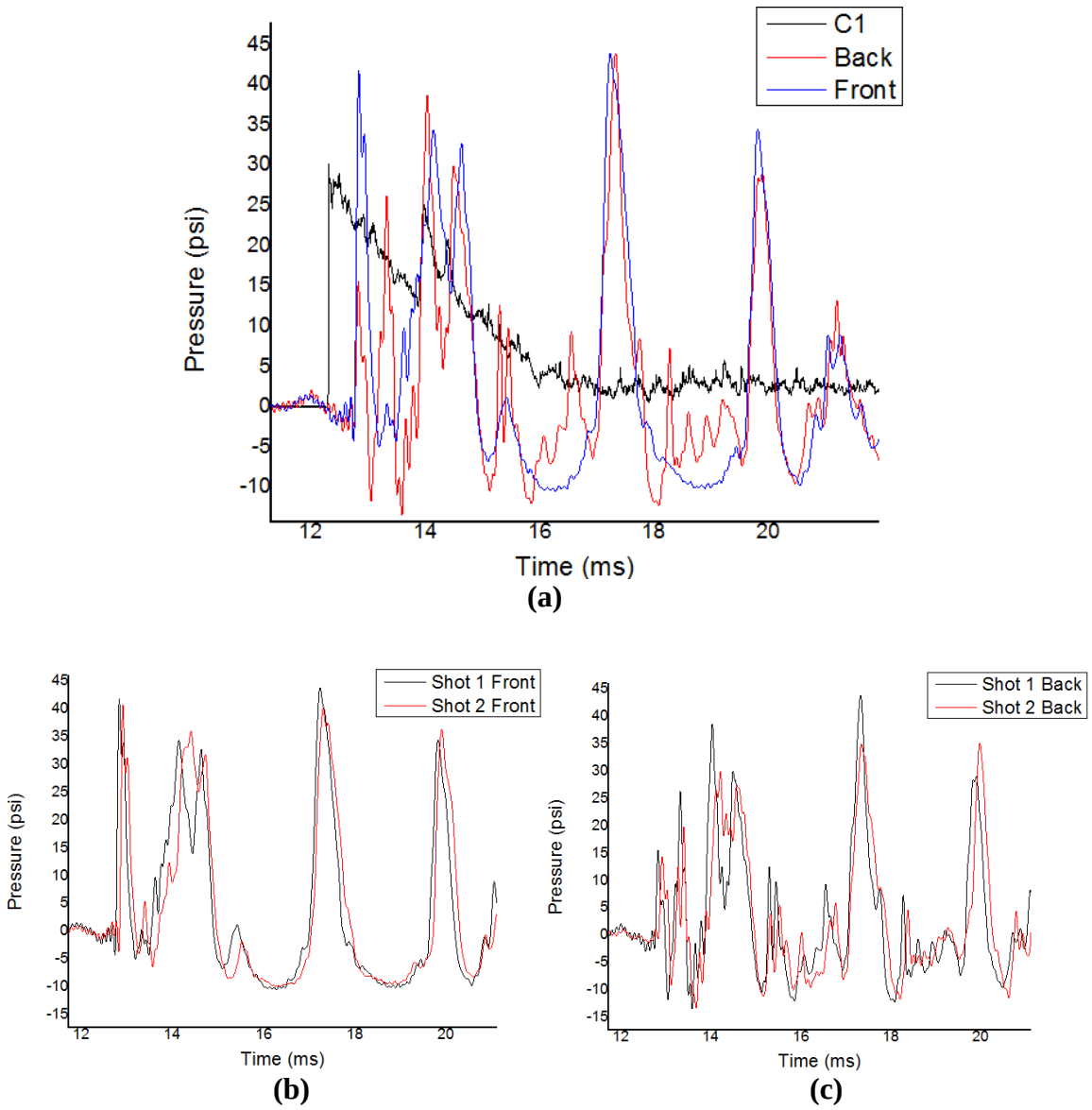

Figure 3.11 Thick cylinder- For incident pressure of 30 psi, pressure profiles of sensors (a) C1, Front and Back (b) Front sensor response (c) Back sensor response for two samples.

For the thick cylinder, it is difficult to investigate the loads applied on cylinder due to directly transmitted waves and the indirect loads because as the thickness of the cylinder is increased, the deflection of the cylinder is reduced. For that reason, the primary peak value is considered to be the resultant of low deformation of the cylinder and the fluid pressure transmitted from the blast loads.

From Figure 3.9, for an incident pressure of 20 psi, the primary peak value of front sensor is observed to be 14 psi whereas it is approximately 34 psi in the thin cylinder. This low peak value is due to decreased deflection of cylinder because of the increase in thickness. As the wave travels inside the fluid, the back sensor peak value is further decreased to 10 psi whereas for the thin cylinder the peak value is 14 psi.

For incident pressure of 30 psi, the peak value reading from front sensor is 39 psi, which is less when compared to thin cylinder, which is 48 psi. As the wave moves towards back sensor, its peak value decreases to 13 psi whereas for the thin cylinder with same incident pressure it is 15 psi.

Table 3.2 Primary Peak Value Comparison between Thin and Thick Cylinders

Kulite Sensor Location	20 psi		30 psi	
	Thin	Thick	Thin	Thick
Front	34 psi	14 psi	48 psi	40 psi
Back	14 psi	10 psi	15 psi	13 psi

Although we considered primary peak value of thick cylinder to be both direct and indirect loads, the pressure value is still less when compared to thin cylinder. This clearly proves that the thickness of the cylinder has major contribution in transferring the direct and indirect loads inside the fluid which is considered as brain material.

3.5 Deformations Due to Blast Loading

When blast loads are applied on a circular cylinder, the shape will be transformed into an ellipse. The front and back of cylinder will be compressed forming the minor axis of the ellipse whereas the sides of the circular cylinder will be transformed into the major axis. The transformation from a circular cross section to an elliptical one is due to compression applied on the front of the cylinder, which causes increased tension on the side of the cylinder and subsequent compression of the back of the cylinder.

Deformations depend majorly on shell thickness: as the thickness of the shell increases the deformation decreases (10). To observe the amount of compression and tension, three strain gauges are placed on front, side and back of cylinder. Strain gauges are so sensitive that, when attached to the test specimen, even when small load is applied, the grid pattern will elongate causing a resistance change in the wheat stone bridge and a voltage change, used to calculate strain. So, by using strain gauges, deformations occurring at micro level on the polycarbonate cylinder surface can be captured. Strain is nothing but the change in deformation before and after applying loads. The strain is defined as follows:

$$\varepsilon = \frac{\Delta l}{l}$$

where ε is strain, Δl is change in length and l is original length.

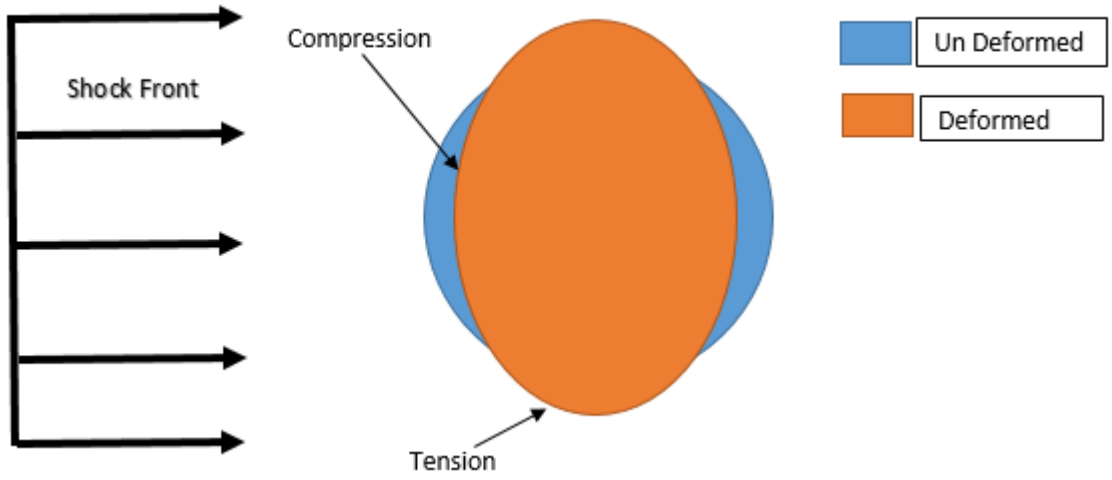

Figure 3.12 Circular cylinder transformation into elliptical cylinder due to blast loads.

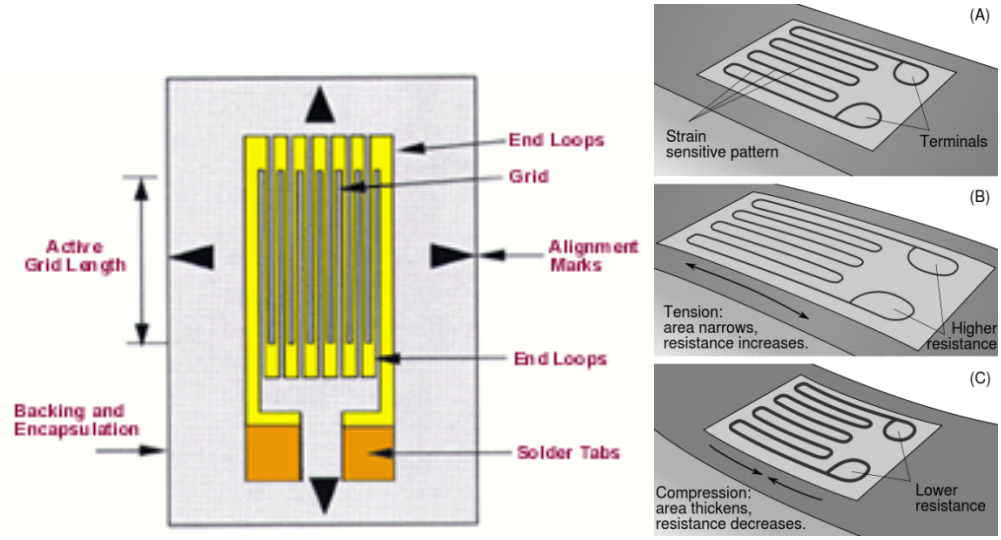

(a) **(b)**

Figure 3.13 (a) Detailed view of linear Strain gauge. (b) Working concept of strain gauge on bending.
Source: www.sensorland.com , en.wikipedia.org/wiki/Strain_gauge

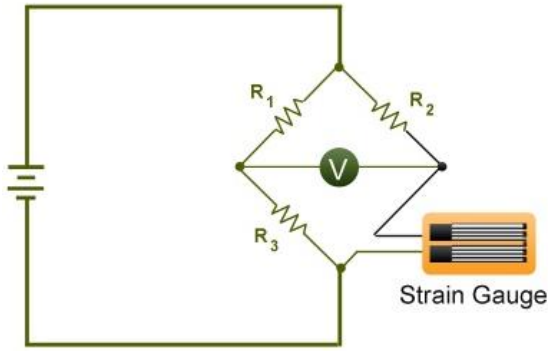

Figure 3.14 Wheatstone quarter bridge circuit with strain gauge.
Source: Chipkin Automation Systems Inc.

The Wheatstone quarter bridge is connected to amplification circuit to amplify the voltage output as the original output from the strain gauges will be in micro level. The resistances in the Wheatstone bridge will be adjusted in such a way that the voltage output will be set to zero before applying load on the specimen.

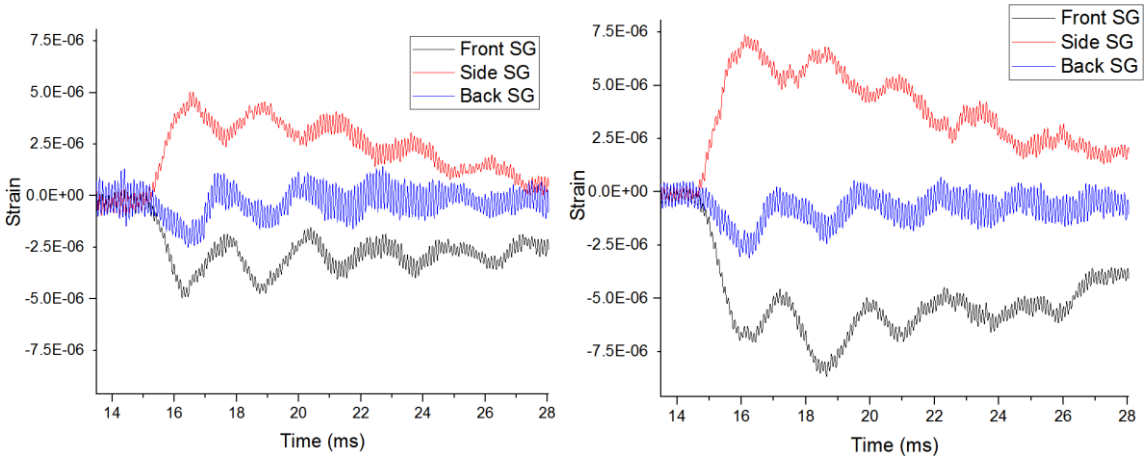

(a) **(b)**

Figure 3.15 Strain gauge output values for front, side and back of thin cylinder (a) 20 psi (b) 30 psi.

The strain output from the graph (Figure 3.15) showing the response of the strain gauges when exposed to blast loadings show positive value for the side sensor and

negative value for front and back sensors. This is because of the effect of compression on front and back of cylinder and tension on the side of cylinder.

The hypothesis is that the back and front of the cylinder should show equal amounts of compression. But due to the tubings and adhesives used to keep them in place, the back of cylinder was stiffer resulting in less deflection. Comparison between the tension on the side and front show approximately equal forces. Observed strains are at the micro level and consequently, the difference between different incident pressures and thickness of the cylinder will also be in micro level.

3.5.1 Strain Comparison for Thin and Thick Cylinder at Different Incident Pressures

The strain comparison helps to better understand the small differences of strains observed on the specimen. From the Figure 3.16, the differences between thin and thick cylinders are compared for better understanding of the effect of indirect loads applied on the fluid due to deformations of cylinder.

This clearly shows that the deformations on the cylinder change with the thickness of cylinder and incident pressure. For the thin cylinder with 20 psi blast load condition, the strain gauge output shows a greater peak when compared to 30 psi load. And when compared with a 20 psi load applied on thick cylinder, the effect of deformation is observed to be reasonably low. At an incident pressure of 20 psi, there wasn't significant difference in deformations, but when the incident pressure was increased to 30 psi, a very noticeable difference was observed between thick and thin cylinders.

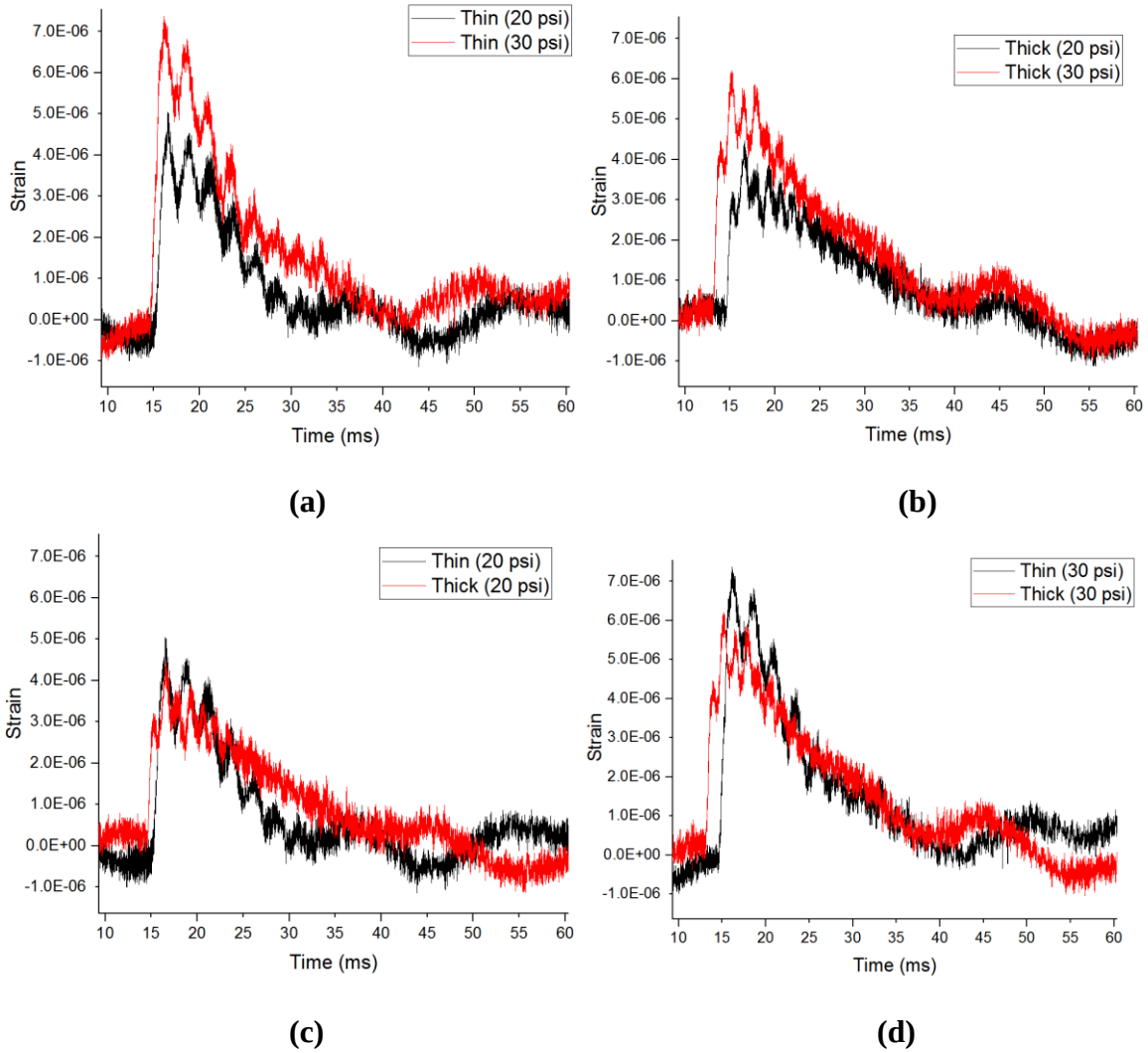

Figure 3.16 Strain output comparison of side strain gauge for thin and thick cylinders at different incident pressures.

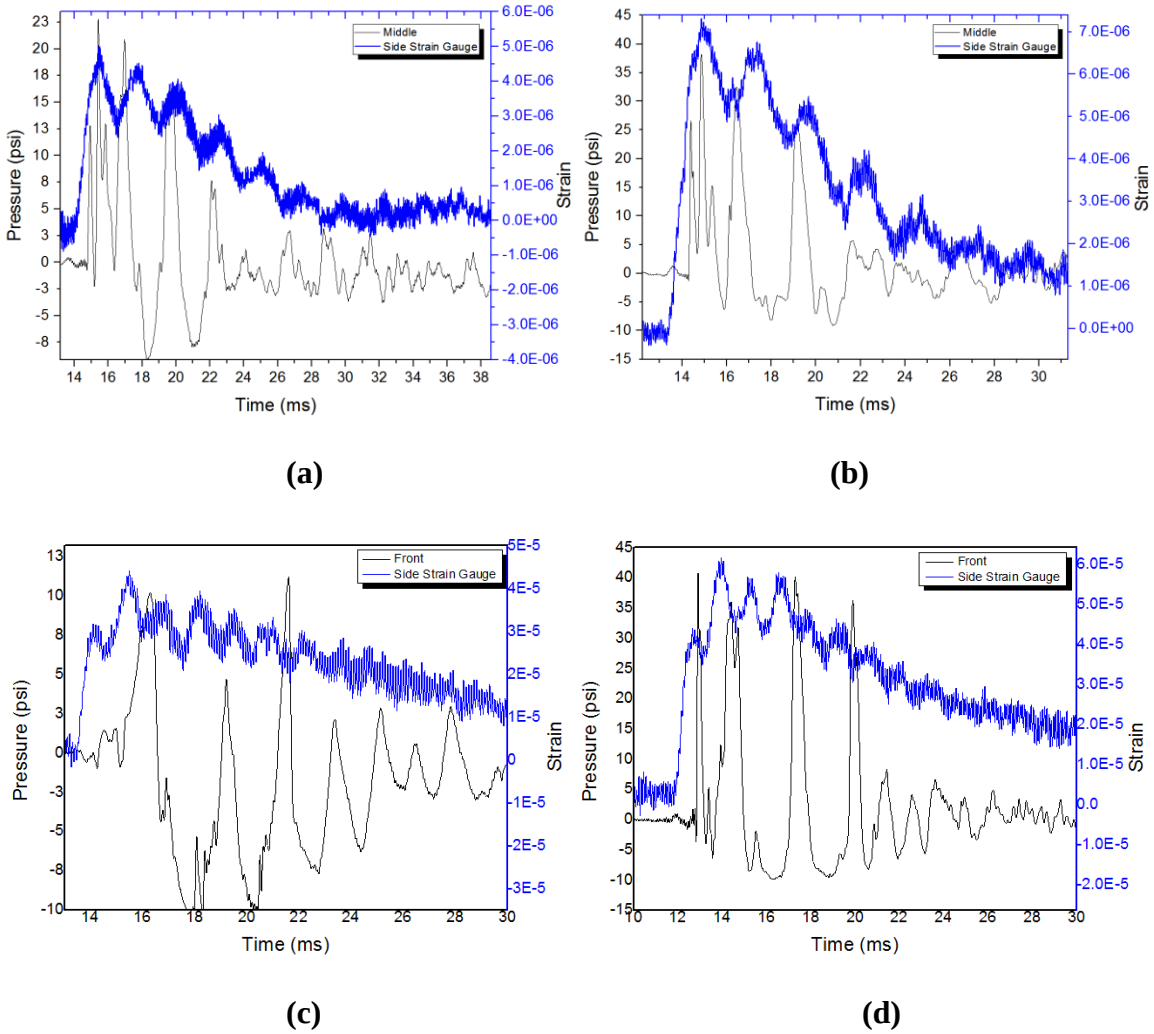

Figure 3.17 Strain gauge output and pressure profile comparison (a) 20 psi incident pressure, thin cylinder (b) 30 psi incident pressure, thin cylinder (c) 20 psi incident pressure, thick cylinder (d) 30 psi incident pressure , thick cylinder.

Figure 3.17 (a) and (b), explains comparison between middle kulite sensor response and side strain gauge response. The side strain gauge responds approximately 1 ms before middle kulite because of the acoustic velocity of polycarbonate (2270 m/s) is higher than for water (1482 m/s). The strain gauge response shows that loading increases uniformly before reaching peak value. The secondary peak in the middle kulite sensor and primary peak of side strain gauge reaches maximum value at same time (15.5 ms). This clearly explains that the second peak has major effect of deformation (maximum loading) of the cylinder.

Figure 3.17 (c) and (d) is comparison between strain output of side strain gauge and front kulite pressure output at different incident pressures for thick cylinder. From strain gauge response, it is observed that loading is not uniform. The cylinder is deforming slightly before it reaches maximum bending (peak value in strain gauge). This effect is due to the thickness of the cylinder where the stress wave passing through the cylinder wall before it reaches maximum value. Because of this slight deformation due to stress wave, it is hard to differentiate the peak due to transmitted fluid pressure and the deflection of cylinder. For this reason, the primary peak is considered as a result of both fluid pressure and slight deformation. Though the primary peak of thick cylinder is considered as because of both transmitted fluid pressure and slight deflection of cylinder, the primary peak over pressure is slightly less for thick cylinder when compared to thin cylinder.

CHAPTER 4

CONSLUSION AND SUMMARY

The primary goal of this project is to investigate the difference in the pressure response inside cylinders with different thicknesses. Cylinders are representative of human skull material and the water inside, brain material. The cylinder is exposed to different blast load conditions with incident pressures of 20 and 30 psi. The cylinder is allowed to move in one direction up to certain fixed point in order to better simulate free field conditions.

From the results discussed in Chapter 3, the comparison between moving cylinder and stationary cylinder of same thickness and diameter states that, when cylinder is moving, the deflections obtained are less when compared to stationary cylinder. For a moving cylinder, when blast loads are applied on cylinder, some energy will be used to push the cylinder and some energy will be transmitted inside cylinder, but when cylinder is stationary all the energy will be transferred into cylinder wall, allowing more deflection resulting in more indirect loads transmitted inside fluid.

As the human skull vary in thickness from 4 mm in temporal region to 8 mm in occipital region, two different thickness cylinders are compared. Although skull thickness vary from person to person and also vary from gender to gender, we selected two different thicknesses for the purpose of this experiment.

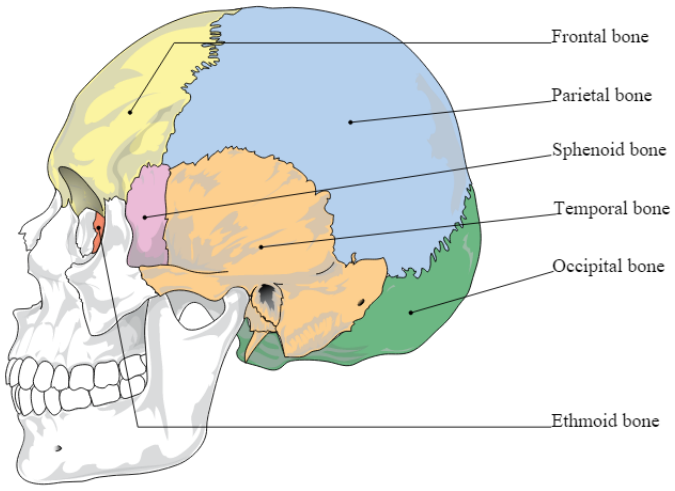

Figure 4.1 Different regions of bones in skull (side view).
Source: Anatomy and Physiology textbook published by Boundless, 2013 edition

Table 4.1 Variation of Skull Thickness at Different Bone Segments (11)

Skull Bone Segment	Thickness (mm)
Frontal	7
Temporal	4
Occipital	8
Parietal	6

As the thickness of cylinder increased, the indirect loads caused due to the deformation reduced, thereby the pressure observed was lower when compared to thin cylinder. As the thickness increases, the transmitted wave pressure decreases; it has not been observed much due to small differences between the thin and thick cylinders considered for this thesis work (1.9mm and 3.3mm).

4.1 Limitations

Although the results offer some differences to compare, there are some limitations needed to be considered,

1. The cylinder selected for this purpose is polycarbonate which has mechanical properties close to bone material, but the geometry of skull is different. The circular cylinder is just considered for idealization purposes only.
2. When an object is subjected to blast loads, many reflections takes place which are not considered for this thesis work as our primary interest is pressure variance inside the fluid.
3. The output observed from different sensors show some negative phase of pressure which is not much considered in detail.

4.2 Further Scope

1. Only two thicknesses of same diameter are considered for this project. Different thicknesses and different diameters cylinders can be used to study variation of pressure response inside the fluid.
2. We can also analyze the phenomenon of cavitation formation and implosion, one of the proposed mechanisms of blast induced traumatic brain injury. This experimental set up lends itself to observation of these bubbles and analysis of their loading effects.
3. All the results obtained are experimentally valid, these values can be compared with simulated results using flow analysis software like ABACUS © or ANSYS©.

REFERENCES

Ruff RL, Ruff SS, Wang X-F. "Headaches among operation Iraqifreedom/operation enduring freedom veterans with mild traumatic brain injury associated with exposures to explosions." J Rehabil Res Dev (2008) 45:941–52. doi:10.1682/JRRD.2008.02.0028

Teasdale G, and Jennett, B, 1974, "Assessment of Coma and impaired consciousness: A Practical Scale", The Lancet.

Bir, C., 2011, "Measuring Blast – Related intracranial Pressure within the Human head", Final Report, U.S. Army medical Research and material command, Award No. W81XWH-09-1-0498.

Kinney GF, Graham KJ. "Explosive Shocks in Air" New York, NY: Springer-Verlag, Second edition (1985). DOI 10.1007/978-3-642-86682-1.

Chen X and Chandra N, 2004, "The Effect of Heterogeneity on Plane Wave Propagation through Layered Composites," Compos. Sci. Technol., 64(10–11), pp. 1477–1493.

Chen X, Chandra N., and Rajendran, A. M., 2004, "Analytical Solution to the Plate Impact Problem of Layered Heterogeneous Material Systems," Int. J. Solids Struct., 41(16–17), pp. 4635–4659.

Acoustic impedance, http://www.schoolphysics.co.uk/age16-19/Sound/text/Acoustic_impedance/index.html.

Sundaramurthy A, Chandra N. "A parametric approach to shape fieldrelevant blast wave profiles in compressed-gas-driven shock tube." Frontiers in Neurology, volume 5, Article 253, doi:10.3389/fneur.2014.00253, 2014.

Chandra N and Sundaramurthy A. "Acute Pathophysiology of Blast Injury-From Biomechanics to Experiments and Computations: Implications on Head and Polytrauma." page 196-251, Brain Neurotrauma: Molecular, Neuropsychological and Rehabilitation Aspects, Ed. Firas. H. Kobeissy, CRC Press, ISBN 9781466565982 - CAT# K16127, Frontiers in Neuroengineering Series.

Anderson J D, "Fundamentals of Aerodynamics", (Mc Graw-Hill, New York, 2001)

Baer, Melvyn J, Harris, James E. "A commentary on the growth of the human brain and skull". *Am J Phys Anthropol*. 1969;30:39–44